# Reactivities of Substituted *α*-Phenyl-*N-tert*-butyl Nitrones

Marie Rosselin,[†,‡] Fanny Choteau,[†,‡] Kamal Zéamari,[§] Kevin M. Nash,[‖,⊥] Amlan Das,[‖,⊥] Robert Lauricella,[§] Elisabeth Lojou,[¶] Béatrice Tuccio,[§] Frederick A. Villamena,*[,‖,⊥] and Grégory Durand*[,†,‡]

[†]Avignon Université, Equipe Chimie Bioorganique et Systèmes Amphiphiles, 33 rue Louis Pasteur, F-84000 Avignon, France

[‡]Institut des Biomolécules Max Mousseron (UMR 5247), 15 avenue Charles Flahault, F-34093 Montpellier Cedex 05, France

[§]Aix-Marseille Université-CNRS, Institut de Chimie Radicalaire (UMR 7273), Equipe Spectrométries Appliquées à la Caractérisation Structurale, avenue Escadrille Normandie-Niemen, F-13397 Marseille Cedex 20, France

[‖]Department of Pharmacology and [⊥]The Davis Heart and Lung Research Institute, College of Medicine, The Ohio State University, Columbus, Ohio 43210, United States

[¶]CNRS-Aix-Marseille Université, Bioénergétique et Ingénierie des Protéines (UMR 7281), 31 chemin Joseph Aiguier, F-13402 Marseille Cedex 20, France

**S** *Supporting Information*

**ABSTRACT:** In this work, a series of *α*-phenyl-*N-tert*-butyl nitrones bearing one, two, or three substituents on the *tert*-butyl group was synthesized. Cyclic voltammetry (CV) was used to investigate their electrochemical properties and showed a more pronounced substituent effect for oxidation than for reduction. Rate constants of superoxide radical ($O_2^{•-}$) reactions with nitrones were determined using a UV−vis stopped-flow method, and phenyl radical ($Ph^•$) trapping rate constants were measured by EPR spectroscopy. The effect of *N-tert*-butyl substitution on the charge density and electron density localization of the nitronyl carbon as well as on the free energies of nitrone reactivity with



**Y**: α-substitution
**Z**: β-substitution

$O_2^{•-}$ and $HO_2^•$ were computationally rationalized at the PCM/B3LYP/6-31+G**//B3LYP/6-31G* level of theory. Theoretical and experimental data showed that the rates of the reaction correlate with the nitronyl carbon charge density, suggesting a nucleophilic nature of $O_2^{•-}$ and $Ph^•$ addition to the nitronyl carbon atom. Finally, the substituent effect was investigated in cell cultures exposed to hydrogen peroxide and a correlation between the cell viability and the oxidation potential of the nitrones was observed. Through a combination of computational methodologies and experimental methods, new insights into the reactivity of free radicals with nitrone derivatives have been proposed.
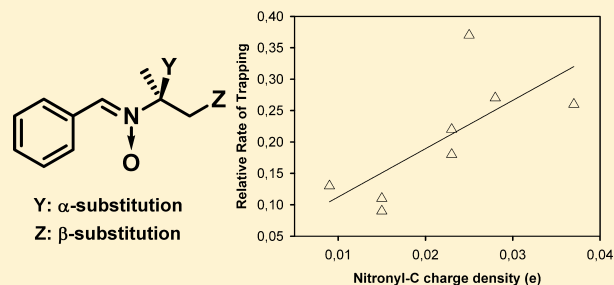
## ■ INTRODUCTION

The addition of free radicals to nitrones yields a persistent aminoxyl-based spin adduct that can be detected and characterized by electron paramagnetic resonance (EPR) spectroscopy. Spin trapping by EPR spectroscopy is a popular method for the detection of free radicals in chemical and biological systems.[1] *α*-Phenyl-*N-tert*-butyl nitrone (PBN) and its derivatives are widely employed as spin traps in in vitro, in vivo, and ex vivo systems.[2,3] Aside from their application as spin traps, nitrones have also exhibited a variety of protective properties in animal models against oxidative stress-mediated injury.[4,5] However, despite the promising pharmacological properties of PBN, the molecular mechanism of its action is not well understood. Of the many PBN derivatives that have been synthesized over the years, disodium [(*tert*-butylimino)methyl]-benzene-1,3-disulfonate *N*-oxide (NXY-059) has gained the most attention since it is the first neuroprotective agent to reach phase 3 clinical trials in the USA.[6] Although it has been suggested that the radical trapping properties of NXY-059 is the basis of its

neuroprotective action, experimental evidence suggest other possible mechanisms are involved.

One of the promising strategies in the design of novel nitrone-based spin traps is to selectively target these compounds in relevant sites of radical production, mainly the mitochondrial electron transport chain, the cytosol, and the membrane-bound NAD(P)H oxidase.[7−9] Selective targeting is usually achieved by conjugating the nitronyl group to specific target ligands, and therefore, the choice of linker groups for optimal spin trapping properties is highly desirable. In addition to the types of ligands that are tethered to nitrones, it has been demonstrated that the nature of the linker group also affects its bioactivity.[10]

Only a relatively limited number of *N-tert*-butyl substituted nitrones have been synthesized over the past few years, with functionalization of the aromatic ring being the most facile method. Several *N-tert*-butyl-substituted PBNs have been

synthesized, such as *N*-benzylidene-1-diethoxyphosphoryl-1-methylethylamine *N*-oxide (PPN),[11] *N*-benzylidene-1,1-bis-(ethoxycarbonyl)ethylamine *N*-oxide (DEEPN),[12] and the amide amphiphilic nitrones developed by our group (LPBNAH),[9] (Figure 1), but the effect of the substituents on



**Figure 1.** General structure and some examples of substituted linear nitrones.

the electronic properties of the nitrones and their reactivity with radicals such as $O_2^{\bullet-}$ are not known. The substituent effect on the reactivity of DMPO-type cyclic nitrones has been extensively studied through experimental and computational approaches,[13−15] demonstrating the nucleophilic nature of $O_2^{\bullet-}$ addition to C-5-substituted DMPO nitrones.[13] Therefore, derivatization of the *tert*-butyl group of the PBN may exhibit electronic properties that enhance $O_2^{\bullet-}$ addition to nitrones and offers opportunities for multifunctionalization of the spin trap for subcellular target specificity and controlled delivery in in vitro and in vivo systems.

Our previous computational and kinetic studies showed that para substitution by electron-withdrawing substituents in PBN

gave no significant polar effects on their reactivity toward $O_2^{\bullet-}$, while with $HO_2^{\bullet}$, a more pronounced increase in the kinetics of addition was observed, indicating the electrophilic nature of this reaction. Our current goal is to explore the reactivity of various *N*-tert-butyl-substituted phenyl nitrones so as to identify the most optimal linker groups. Through optimization of the linkers, we would be able to design selective targeted nitrone-based spin traps with improved reactivity toward free radicals.

In this work, five new *N*-tert-butyl-substituted PBNs were synthesized along with a series of mono-, di-, and trihydroxymethyl *N*-tert-butyl-substituted derivatives. The water solubility, lipophilicity, and electrochemical properties were determined. A UV−vis stopped-flow competitive technique was employed to determine the relative rate constants of reaction with $O_2^{\bullet-}$. The relative rate constants of phenyl adduct formation were experimentally determined by an EPR competition kinetic technique. Using a computational approach, the effect of the *N*-tert-butyl substituents on the nitronyl atom charge density and electron density localization as well as on the free energies of nitrone reactivity with $O_2^{\bullet-}$ and $HO_2^{\bullet}$ were calculated. Finally, the cytoprotective properties of selected compounds against oxidant-induced cell death were investigated.

## ■ RESULTS AND DISCUSSION

**Synthesis of *tert*-Butyl-Substituted Nitrones.** All of the mono-, di-, and trisubstituted nitrones with the substituents in *β*-positions (see Figure 1 for details) were synthesized by a one-pot reduction/condensation of nitro derivatives onto the commercially available benzaldehyde, as shown in Scheme 1. PBN-CH₂OH[16] was synthesized from 2-methyl-2-nitro-1-propanol and benzaldehyde in the presence of zinc powder and AcOH in ethanol according to our recently described procedure.[17] After purification by flash chromatography and two successive crystallizations from EtOAc/*n*-hexane, nitrone **1** was obtained in 65% yield, which is slightly higher than that for the procedure used by Janzen and Zawalsky (55%).[16] Acetylation of nitrone **1** by a 1/1 v/v mixture of Ac₂O and pyridine led to compound **2** (also called PBN-CH₂OAc) in 98% yield, after purification by flash chromatography. The synthesis of compound **3** was carried

**Scheme 1. Synthesis of Mono-, Di-, and Tri-*β*-Substituted Nitrones**[a]



[a]Reagents and conditions: (a) benzaldehyde, zinc powder, AcOH, 4 Å molecular sieves; ethanol, 15 → 60 °C, 10 h; (b) Ac₂O/pyr (1/1 v/v), room temperature, 12 h; (c) DCI, DMAP, THF, 2 h, room temperature, then CH₃NH₂, 18 h, room temperature.

**Table 1. Physicochemical and Electrochemical Properties of PBN Derivatives**

| compd | water solubility (g/L) | lipophilicity | | $E_p(c)$ (V) | | | $E_p(a)$ (V) in CH$_3$CN$^e$ |
| | | | | in H$_2$O$^d$ | in CH$_3$CN$^e$ | | |
| | | log $k'_w$$^b$ | C log $P$$^c$ | | 2nd peak | 1st peak | |
|---|---|---|---|---|---|---|---|
| PBN-CH$_2$OH (**1**) | >200 | 1.35 | 1.61 | −1.70 | −2.12 | −1.92 | 1.57 |
| PBN-CH$_2$OAc (**2**) | nd$^a$ | 1.89 | 2.05 | −1.69 | −2.40 | −2.03 | 1.67 |
| PBN-CH$_2$OCONHMe (**6**) | 10.8 | 1.41 | 1.94 | −1.71 | −2.14 | −1.96 | 1.77 |
| PBN-CH$_2$NHAc (**7**) | >200 | 1.37 | 1.32 | −1.70 | −2.15 | −1.97 | 1.44 |
| PBN-(CH$_2$OH)$_2$ (**8**) | >200 | 0.95 | 0.57 | −1.74 | −2.29 | −2.12 | 1.55 |
| PBN-(CH$_2$OH)$_3$ (**9**) | 21.4 | 0.85 | −0.48 | −1.67 | −2.27 | −2.08 | 1.58 |
| PBN-(CH$_2$OAc)$_2$ (**10**) | nd$^a$ | 1.95 | 1.45 | −1.72 | −2.31 | −1.93 | 1.76 |
| PBN-(CH$_2$OAc)$_3$ (**11**) | nd$^a$ | 2.17 | 0.84 | −1.75 | −2.28 | −1.89 | 1.83 |
| PBN | 21.4 | 1.64 | 2.66 | −1.70 | −2.23 | −2.10 | 1.60 |

$^a$Not determined. $^b$Partition coefficient values obtained by HPLC. $^c$Calculated octanol/water partition coefficient values obtained using Marvin software (http://www.chemaxon.com/marvin/help/index.html). $^d$Containing 50 mM of NaCl. $^e$Containing 50 mM of TBAP.

out in one step. First, 2-methyl-2-nitro-1-propanol was activated using 1,1′-carbonyldiimidazole (CDI) in the presence of 4-dimethylaminopyridine (DMAP) in THF, and then methylamine was added to the reaction mixture to give compound **3** after purification in 98% yield. In parallel, 2-methyl-2-nitro-propanamine (**4**) was obtained from 2-methyl-2-nitro-1-propanol in three steps[9] and was then acetylated to give the nitro compound **5** in 94% yield. The one-pot reduction/condensation of compounds **3** and **5** to benzaldehyde after purification by flash chromatography and two successive crystallization from EtOAc/n-hexane led to nitrones **6** (also called PBN-CH$_2$OCONHMe) and **7** (also called PBN-CH$_2$NHAc) in 70% and 68% yields, respectively.

Following the same synthetic procedure, PBN-(CH$_2$OH)$_2$ (**8**) was also synthesized from 2-methyl-2-nitro-1,3-propanediol in 65% yield, which corresponds to a significant improvement in comparison to the procedure used by Janzen and Zawalsky with 15% yield.[16] PBN-(CH$_2$OH)$_3$ (**9**) was obtained following our recent procedure from 2-hydroxymethyl-2-nitro-1,3-propanediol.[17] Finally, PBN-(CH$_2$OAc)$_2$ (**10**) and PBN-(CH$_2$OAc)$_3$ (**11**) were obtained by acetylation of nitrones **8** and **9**, respectively.

**Water Solubility and Partition Coefficient.** Nitrones **1**, **7**, and **8** are soluble in water up to a concentration of ∼200 g/L, after which the solution became viscous but remained transparent. This is significantly higher than the solubility limit of PBN, which was found to be ∼21 g/L. When the amide and carbamate derivatives **7** and **6** are compared, a significant difference was noted, with **6** exhibiting a water solubility limit of ∼11 g/L. Carbamates are indeed known to be hardly soluble in water.[18] We also demonstrated that the solubility of hydroxylated compounds did not linearly correlate with the number of hydroxyl groups. Whereas the mono- and disubstituted hydroxyl compounds are highly soluble in water (>200 g/L), the trisubstituted compound reaches its solubility limit at ∼21 g/L, likely due to intramolecular hydrogen bonding between the three hydroxyl groups as previously observed.[17] Due to the oily form of the three ester derivatives, their solubility was not determined.

The relative lipophilicity (log $k'_w$) of the nitrones was measured by HPLC, and values are reported in Table 1. This confirms the higher lipophilic character of the three ester compounds in comparison to that of PBN with log $k'_w$ values of 1.89, 1.95, and 2.17 for compounds **2**, **10**, and **11**, respectively, whereas a value of 1.64 was found for PBN. Although compounds **6** and **7** exhibit different water solubilities, they

were both found to have similar lipophilicities, slightly lower than that of PBN. Finally, the hydroxylated derivatives **1**, **8**, and **9** were found to be the least lipophilic derivatives, where the lipophilicity correlates with the number of hydroxyl groups: that is, the lower the number of hydroxyl groups, the higher the lipophilicity. Calculated partition coefficients (C log $P$) were also determined using Marvin software. Except for the three ester derivatives, a good correlation between log $k'_w$ and C log $P$ was obtained (Figure S1, Supporting Information).

**Spin Trapping.** To evaluate the spin trapping ability of the PBN-substituted derivatives, we investigated the formation of various oxygen-centered radical spin adducts: i.e., HO$^•$, O$_2^{•−}$, and MeO$^•$ adducts. The hyperfine coupling constants (hfccs) of the monosubstituted derivatives **1**, **2**, **6**, and **7** and those of the di- and trihydroxylated derivatives **8** and **9** are reported in Table 2. In most cases, the nitrones tested gave rise to a standard six-line EPR spectrum whose values are in agreement with those in the literature.[19] Two different conditions were used to generate the superoxide adducts: that is, pyridine/H$_2$O$_2$ and DMSO/KO$_2$. In the pyridine/H$_2$O$_2$ system, one predominant radical adduct was detected in most cases with hfcc values in agreement with a O$_2^{•−}$ adduct. In the KO$_2$ system, the hyperfine coupling constants suggest O$_2^{•−}$ adduct formation with values higher than those in the pyridine/H$_2$O$_2$ system, which is likely due to solvent effects, as previously observed for para-substituted nitrones.[20] For the hydroxylated derivatives, the presence of a second nitroxide having a six-line pattern spectrum was also observed. This second species corresponds to an oxazolidine-N-oxyl compound coming from a cyclization reaction between one hydroxyl group and the nitronyl carbon.[17]
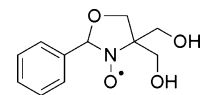


Under Fenton conditions, the ratio of the cyclic species increased with the number of hydroxyl groups: ∼1:3 for compound **1** ($a_N$ = 15.9, $a_H$ = 20.1) and ∼2:3 for compound **8** ($a_N$ = 15.6, $a_H$ = 19.9), while for compound **9** bearing three hydroxyl groups ($a_N$ = 15.3, $a_H$ = 19.7), the cyclic species was predominant (>90%). This suggests that cyclization may be favored with an increasing number of hydroxyl groups, and a thorough investigation on this is currently in progress in our laboratories. The formation of five-membered cyclic nitroxides was also evident in the KO$_2$ system for the hydroxylated derivatives; however, in this case, the ratio of the cyclic nitroxide

**Table 2. EPR Hyperfine Coupling Constants of Different Radical Adducts of β-Substituted Nitrones**

| radical adduct | source | solvent | PBN-CH₂OH (1) $a_N$ | $a_H$ | ratio | PBN-CH₂OAc (2) $a_N$ | $a_H$ | PBN-CH₂OCONHMe (6) $a_N$ | $a_H$ | PBN-CH₂NHAc (7) $a_N$ | $a_H$ | ratio | PBN-(CH₂OH)₂ (8) $a_N$ | $a_H$ | ratio | PBN-(CH₂OH)₃ (9) $a_N$ | $a_H$ | ratio |
|---|---|---|---|---|---|---|---|---|---|---|---|---|---|---|---|---|---|---|
| HO• | Fenton | PBS | 15.5 / 15.9 | 2.5 / 20.1 | 2:3 / 1:3 | 15.2 | 2.8 | 15.2 | 2.9 | 15.1 | 2.9 | | 15.2 / 15.6 | 2.4 / 19.9 | 1:3 / 2:3 | 15.3 | 19.7 | |
| O₂•⁻ | KO₂ | DMSO | 14.9 / 14.2 | 17.9 | 2:3 / 1:3 | 14.0 | 1.6 | 14.9 | 0.4 | 14.6 / 13.6 | 16.5 / 2.4 | 1:2 / 1:2 | 14.7 / 14.9 | 2.8 / 18.1 | 2:3 / 1:3 | 14.5 / 14.6 | 2.3 / 18.5 | 3:4 / 1:4 |
| HOO• | H₂O₂ | pyridine | 13.3 | 1.5 | | 13.1 | 1.4 | 13.3 | 1.6 | 13.3 | 1.7 | | 13.1 | 1.2 | | 13.1 / 14.1 | 1.1 / 2.0 | 3:4 / 1:4 |
| CH₃O• | MeOH, Pb(OAc)₄ | DMSO | 15.0 / 13.4 | 18.0 / 0.8 | 4:5 / 1:5 | 13.5 | 2.4 | 13.6 | 2.5 | 13.7 | 2.4 | | 13.1 / 12.8 | 0.35 / 1.9 | 1:3 / 2:3 | 12.9 | 2.1 | |
| C₆H₅• | C₆H₅-I/UV | benzene | 14.5 | 2.5 | | 13.6 | 2.2 | 14.4 | 3.0 | 14.1 | 2.3 | | 14.2 | 2.3 | | 14.1 | 2.0 | |

decreased with the number of hydroxyl groups. Cyclization was observed during methoxy radical trapping for the monohydroxylated compound but not for the di- and trihydroxylated derivatives. Regardless of the radical generating system used, no evidence of cyclization was found for the carbamate- and ester-based compounds, while for the amide derivative, cyclization was only evident in the KO₂ system.

We also investigated the trapping of a carbon-centered radical. The phenyl radical spin adduct was obtained by photolysis of a phenyl iodide solution in benzene in the presence of the nitrones. Although all the nitrones tested trapped Ph•, giving rise to a standard six-line EPR spectrum, it should be noted that a weak signal was obtained with the trihydroxylated compound 9. In all cases, $a_N$ and $a_H$ values determined are in agreement with an aryl radical adduct of a PBN-type nitrone.

**Cyclic Voltammetry.** The oxidative and reductive character of these nitrones was investigated using cyclic voltammetry, and values are reported in Table 1. We first carried out cyclic voltammetry in 50 mM NaCl aqueous solution. As already observed for other nitrones, the oxidation of the nitronyl group was not detected.[21,22] In contrast, we observed that all of the nitrones exhibited an irreversible one-step reduction, as shown in Figure S2−S4 (Supporting Information). The cathodic peak potential of the β-substituted derivatives is observed between −1.67 and −1.75 V vs Ag/AgCl, and that of the PBN is at −1.70 V. This is consistent with the findings by Zuman and Exner,[23] who reported the weak influence of N-alkyl substituents on the reduction potential of α-phenyl-N-alkyl nitrones, which was further confirmed by McIntire et al.[21] We next studied the electrochemical properties of the nitrones in acetonitrile containing tetrabutylammonium perchlorate (TBAP) as electrolyte. Previous works showed that PBN undergoes an irreversible one-electron oxidation and a one-step, two-electron reduction.[21,24,25] In comparison to the case for the aqueous conditions, oxidation of nitrones was clearly observed in acetonitrile, as shown in Figure 2 and Figures S5 and S6 (Supporting Information), with values ranging from 1.44 to 1.83 V. For the monosubstituted derivatives, the highest observed oxidation potential was for the carbamate derivative 6 followed by the ester 2 and then by the hydroxylated 1, which suggests a strong inductive effect of the carbamate bond, making nitrone 6 harder to oxidize than nitrones 2 and 1. This shows that the presence of β-substituents affects the oxidation of the nitronyl function. The amide compound 7, with the lowest anodic peak potential in the series, is therefore the easiest to oxidize, demonstrating that the oxidation of the nitronyl group is more difficult in the presence of electron-withdrawing substituents, in agreement with the literature.[21,25] With regard to the number of substituents, the oxidation potential of the ester derivatives 2, 10, and 11 increases with the number of substituents, suggesting that the electronic effects are additive. No significant trend was observed for the mono-, di-, and trihydroxylated derivatives, whose potentials were close to that of PBN, in agreement with the literature.[21]

The reduction of nitrones in a nonaqueous medium was then investigated and exhibited two reduction potentials for all of the β-substituted derivatives, whereas for PBN, only one reduction peak was observed (Figure 2 and Figures S7 and S8 (Supporting Information)). The presence of two reduction potentials had been observed for β-phosphorylated nitrone spin traps.[24] For the monosubstituted derivatives, only a modest ease of reduction was observed in comparison to PBN with only ~0.1−0.2 V shift in potential. The reduction of the ester derivatives becomes slightly easier with increasing numbers of substituents, suggesting an
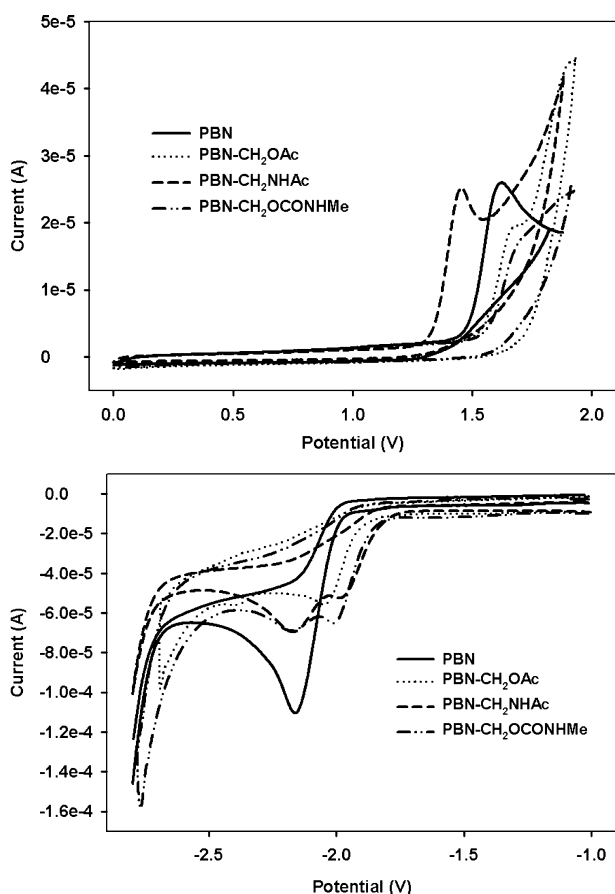
**Figure 2.** Cyclic voltammograms of PBN and compounds **2**, **6**, and **7** in acetonitrile containing 50 mM of TBAP with a sweep rate of 0.1 V s$^{-1}$.

additive effect, as also observed for the oxidation, which is in contrast to the hydroxylated derivatives, where no correlation was found. We further studied the influence of the sweep rate of PBN and compounds **2** and **7** on the anodic and cathodic peak current densities. The linear relationship between the cathodic and anodic peak currents and the square root of the sweep rate, as shown in Figures S9−S11 (Supporting Information), demonstrates that the process is diffusion-controlled.[26,27] The diffusion coefficients of the three nitrones were found to be in the same range for both oxidation and reduction. The reduction of nitrones **2** and **7** exhibited two separate reduction potentials where the current intensity and the square scan speed were linear for both peaks.

**Nitronyl Atom Charge Density Correlation with NMR Chemical Shift.** Examination of the optimized structures at the B3LYP/6-31G* level of theory shows C=N and N−O bond distances that are in the ranges of 1.312−1.317 and 1.276−1.292 Å, respectively, which are consistent with the X-ray crystallographic C=N and N−O bond lengths observed for *N-tert*-butyl-α-(2-pyridyl) nitrone of 1.307 and 1.294 Å, respectively.[28] The natural population analysis (NPA) charges on the nitronyl carbon, nitronyl nitrogen, and nitronyl oxygen atoms were determined at the PCM/B3LYP/6-31+G** level for compounds **1−3** and **5−11** as well as for the other *N-tert*-butyl-substituted derivatives (Table S1, Supporting Information). In general, increasing the number of substituents results in more positive charge densities on the nitronyl C with the exception of a few compounds such as PBN-NHC(=O)Me and PBN-CH$_2$P(=O)(OMe)$_2$, whereas for the nitronyl N, an opposite but less

pronounced trend was observed. As for the nitronyl O, no significant effect of the substitution was observed throughout the series of *N-tert*-butyl-substituted derivatives. This observation is consistent with increased distribution of the mesomeric B form to the resonance hybrid form in the presence of multiple substituents, where there is an increased electron density on the nitronyl N and a decreased electron density on the nitronyl C. This is further supported by natural bond orbital (NBO) analysis, showing that there is a decrease in the percent (0.25−2.97%) of electron localization on the nitronyl C with increasing substitution (from mono to tri) except for PBN-NHC(O)Me and PBN-CH$_2$P(=O)(OMe)$_2$, where there is an increase in electron distribution (Table S2, Supporting Information).
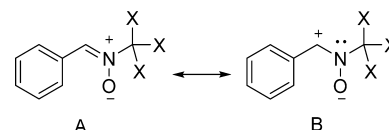


The effect of the nature of the substituent on the charge density of the nitrone moiety was also studied using $^1$H and $^{13}$C NMR spectroscopy. Similar to the case for carbonyl compounds, nitrones are susceptible to nucleophilic addition reactions, and therefore, the electronic nature of the nitronyl C can affect its reactivity toward nucleophilic radicals such as O$_2$$^{\bullet-}$. Figure 3A shows a good correlation between the $^{13}$C NMR chemical shift in CDCl$_3$ of the nitronyl C and the calculated nitronyl C charge density, where there is a downfield shift with increasing positive charge of the nitronyl C. This confirms the presence of a polar effect from the substituent in a β-position on the nitronyl charge density and suggests a stabilization of the mesomeric B form due to the electron-withdrawing effect of the substituents. Only the mono- and dihydroxylated derivatives **1** and **8** were out of the range likely due to the formation of intramolecular hydrogen bonds between the hydroxyl group and the nitronyl O,[17] which may induce a downfield shift. An opposite trend was observed for the $^1$H NMR chemical shift in CDCl$_3$ of the nitronyl H, where an upfield shift of the β-hydrogen was observed with increased positivity of the nitronyl-C, further confirming the polar effect from the *N-tert*-butyl substituents (Figure S12).

**UV−Vis Stopped-Flow Kinetics.** We then applied the UV−vis stopped-flow technique for the determination of the rate constant of the O$_2$$^{\bullet-}$ reaction to nitrones. Phenol red was used as a probe to measure O$_2$$^{\bullet-}$ production, and the rate of formation of this new species at 575 nm is directly proportional to the kinetics of O$_2$$^{\bullet-}$ decay.[13,20] The slope of the linear line generated from the UV−vis absorption plot was used to calculate the rate of nitrone spin trapping by using eq 1, where N is the PBN derivative and $V$ and $v$ are the initial rates of O$_2$$^{\bullet-}$ addition to phenol red (PR) in the absence and presence of PBN derivatives, respectively.

$$V/v - 1 = k_{sN}[\mathrm{N}]/k_{PR}[\mathrm{PR}] \qquad (1)$$

The slopes of the KO$_2$ controls were averaged to give $k_{PR}$. The relative rate constants ($k_{sN}/k_{PR}$) are shown in Table 3, and for comparison, the rates of formation of DMPO and PBN are included. All of the relative rates were significantly lower than 1, demonstrating that O$_2$$^{\bullet-}$ reacts more quickly with phenol red than with the nitrone spin traps. From these values, the $k_{sN}/k_{sPBN}$ ratio was calculated, leading to the following order of increased reactivity to O$_2$$^{\bullet-}$: PBN-(CH$_2$OH)$_2$ < PBN-CH$_2$NHAc < PBN-(CH$_2$OH)$_3$ < PBN-CH$_2$OH < DMPO < PBN-CH$_2$OCONHMe < PBN-CH$_2$OAc. It is worth mentioning that all substituted nitrones exhibit ∼10−50 times higher rates of trapping in
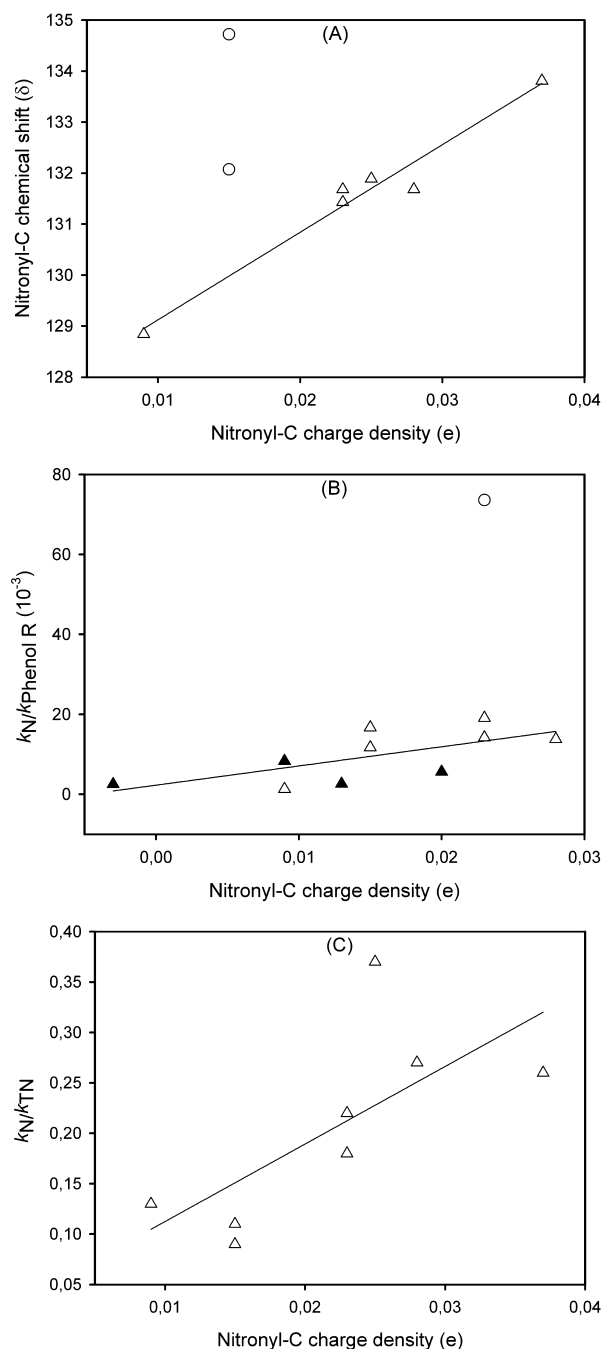
**Figure 3.** Correlation of the nitronyl carbon charge densities with (A) nitronyl C chemical shifts of nitrones **2**, **6**, **7**, **10**, **11**, and PBN ($R^2 = 0.965$), excluding nitrones **1** and **8** (marked as ○) and **9** (which is not soluble in CDCl$_3$), (B) experimental relative rate constants of O$_2^{\bullet-}$ addition to nitrones ($k_{sN}/k_{PR}$), including para-substituted nitrones (marked as ▲) from Durand et al.[20] ($R^2 = 0.451$) and excluding nitrone **2** (marked as ○), and (C) experimental relative rate constants of phenyl addition to nitrones ($k_{pN}/k_{TN}$) ($R^2 = 0.504$).

comparison to PBN. As shown in Figure 3B, the plot of the rate constant of the O$_2^{\bullet-}$−nitrone reaction with the nitronyl-C charge density shows increased rates of reaction for the more positively charged carbons, however, with a fairly poor correlation coefficient. For the sake of comparison, we also plotted the data for para-substituted nitrones.[20] The correlation for para-substituted nitrones is even weaker, which caused us to conclude in our previous work that O$_2^{\bullet-}$ addition to nitrone

**Table 3. Relative Rate Constants for O$_2^{\bullet-}$ and Ph$^\bullet$ Adduct Formation**

| nitrone | UV−vis[a] | | EPR[b] | |
|---|---|---|---|---|
| | $k_{sN}/k_{PR}$ ($10^{-3}$) | $k_{sN}/k_{sPBN}$ | $k_{pN}/k_{TN}$ (±0.05) | $k_{pN}/k_{pPBN}$ |
| PBN-CH$_2$OH (**1**) | 16.7 ± 0.6 | 12.8 | 0.09 | 0.68 |
| PBN-CH$_2$OAc (**2**) | 73.6 ± 0.7 | 56.6 | 0.18 | 1.37 |
| PBN-CH$_2$OCONHMe (**6**) | 19.1 ± 0.3 | 14.7 | 0.22 | 1.66 |
| PBN-CH$_2$NHAc (**7**) | 13.8 ± 0.2 | 10.6 | 0.27 | 2.01 |
| PBN-(CH$_2$OH)$_2$ (**8**) | 11.7 ± 0.4 | 9.0 | 0.11 | 0.80 |
| PBN-(CH$_2$OH)$_3$ (**9**) | 14.2 ± 0.1 | 10.9 | nd[c,d] | nd[c,d] |
| PBN-(CH$_2$OAc)$_2$ (**10**) | nd[c] | nd[c] | 0.37 | 2.79 |
| PBN-(CH$_2$OAc)$_3$ (**11**) | nd[c] | nd[c] | 0.26 | 1.94 |
| **PBN** | 1.3 ± 0.0 | | 0.13 | |
| DMPO | 17.6 ± 0.5 | 13.5 | nd[c] | nd[c] |
| **TN** | nd[c] | nd[c] | | 7.58 |

[a]Ratio of the second-order rate constants for the superoxide radical reaction with various nitrones ($k_{sN}$) and with PBN ($k_{sPBN}$) in DMF/KO$_2$. [b]Ratio of the second-order rate constants for the phenyl radical trapping by various nitrones ($k_{pN}$) and by PBN ($k_{pPBN}$) in benzene. [c]Not determined. [d]The EPR signal of the adduct **9**-Ph was too weak to allow a reliable determination of the ratio.

might be weakly electrophilic. With more compounds included in this study, the trend may suggest a nucleophilic nature of O$_2^{\bullet-}$ addition to this set of nitrones, although the correlation is not satisfactory. This may also suggest that the reaction of O$_2^{\bullet-}$ to nitrone is not charge-controlled but rather orbital-controlled and, hence, warrants further investigation.

**Spin Trapping Kinetics.** Since some nitrones in the series were poorly water soluble or were found to be highly reactive toward HO$^\bullet$, the use of a Fenton system was precluded. Therefore, we chose to study phenyl radical (Ph$^\bullet$) trapping in benzene, where the corresponding adducts show high stability. 1,3,5-Tris[(*N*-(1-diethylphosphono)-1-methylethyl)-*N*-oxyaldimine]benzene (TN)[29] was used as a competitive scavenger to examine the relative rates of trapping by the nitrones **1**, **2**, and **6**−**11** in comparison to PBN (Figure 4). It is worth noting that the adduct decay must be slow enough to be neglected to obtain reliable results with this approach.[30] The Ph$^\bullet$
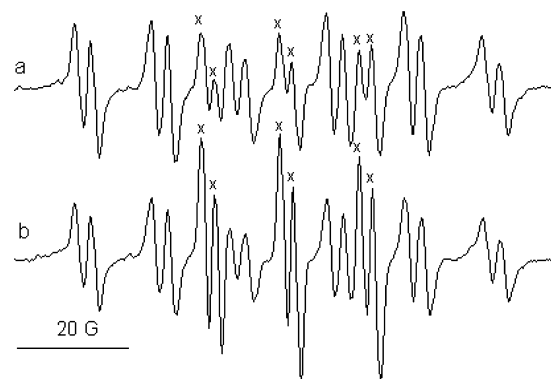


**Figure 4.** EPR signals recorded in benzene by photolysis of 3 mol L$^{-1}$ phenyl iodide solution in the presence of the nitrones **10** and **7** at two different ratios [**10**]/[TN]: (a) [**10**]/[TN] = 0.67 ([**10**] = 20 mmol L$^{-1}$ and [TN] = 30 mmol L$^{-1}$); (b) [**10**]/[TN] = 2 ([**10**] = 40 mmol L$^{-1}$ and [TN] = 20 mmol L$^{-1}$). The peaks marked with × correspond to the phenyl radical adduct of **10**, while the other lines correspond to the phenyl radical adduct of TN.

was generated by UV photolysis of a solution containing a large excess of iodobenzene in the presence of TN and of the nitrone of interest, denoted as N. As previously observed,[29] the possibility of multiple trapping by TN was neglected, since the polyadducts were never observed by EPR in our study. In this method, the Ph[•] spin trapping rate was monitored by measuring the intensities (as the signal area) of the EPR signals of the corresponding adducts. The standard kinetic competition model employed as described elsewhere[29] yielded eq 2. In this equation, the second-order rate constants for Ph[•] trapping by the nitrones N and TN are denoted as $k_{pN}$ and $k_{TN}$, respectively, while $r$ and $R$ represent the trapping rate by TN only in the presence of N and by both TN and N, respectively.

$$R/r = 1 + k_{pN}[N]/k_{TN}[TN] \qquad (2)$$

By plotting the $R/r$ ratio as a function of the $[N]/[N]$ ratio for each nitrone **1**, **2**, and **6−11**, a straight line was obtained with a slope equal to $k_{pN}/k_{TN}$. Five experiments were performed at five different $[N]/[TN]$ ratios kept between 1 and 4. The commercially available PBN was then employed instead of N in order to determine the $k_{pPBN}/k_{TN}$ ratio. From these results, the $k_{pN}/k_{pPBN}$ ratio was calculated and the values obtained for nitrones **1**, **2**, and **6−11** are reported in Table 3.

Though all the nitrones studied were found to be less efficient than the tris(phosphorylated nitrone) TN, many of the substituted PBNs trapped Ph[•] significantly faster than PBN itself, where only the hydroxylated compounds exhibited trapping rates slower than that of PBN. It should be mentioned that the EPR signal of the phenyl radical adduct on **9** was much too weak to permit a reliable evaluation of $k_{pN}/k_{TN}$. This could be due to a much lower trapping efficiency of **9** and/or to a more rapid decay of the spin adduct. Actually, it turned out that the Ph[•] adducts of the hydroxylated nitrones exhibited faster decay than those of other nitrones, and this was more particularly evident in the case of **9**. This observation suggests that the hydroxyl groups would intervene in the nitroxide decay mechanism. The most efficient compounds in the series for trapping Ph[•] are the di- and triacetylated nitrones **10** and **11** and the amide derivative **7**, while the least effective were PBN and the di- and monohydroxylated nitrones **8** and **1**. Similar to what was observed for the stopped-flow kinetics experiments, the rates of reaction correlate with the nitronyl-C charge density, where reasonable correlation can be observed with Ph[•] (Figure 3C). The increased rate of trapping by $β$-substituted nitrones with increasing positive nitronyl-C charge density suggests a nucleophilic nature of the Ph[•] addition to the nitronyl carbon atom. It has been shown that an electron-withdrawing substituent on the aromatic ring of PBN-type compounds increases the reactivity of the nitronyl group for nucleophilic addition reactions and nucleophilic radical addition.[31,32] In contrast, PBN-type nitrones bearing an electron-donating substituent have also been suggested to exhibit high reactivity to electrophilic radicals.[33,34] In this work the polar effect of the N-tert-butyl substituents is obviously electron-withdrawing with hydroxyl, ester, amide, and carbamate groups, which therefore may favor nucleophilic addition. This is in agreement with the findings by Sueishi et al., who suggested the nucleophilic nature of phenyl radical addition to nitrones.[31] More recently De Vleeshouwer et al. confirmed the moderate nucleophilic character of the phenyl radical using natural population analysis.[35]

**Thermodynamics of Adduct Formation.** Examination of the optimized structures at the B3LYP/6-31G(d) level of theory of various spin adducts show $C_{nitronyl}$−N and N−O bond

distances of 1.280−1.292 and 1.472−1.513 Å, respectively, consistent with the X-ray crystallographic $C_{nitronyl}$−N and N−O bonds observed for the phenyl radical adduct of N-tert-butyl-α-(2-pyridyl) nitrone with bond distances of 1.287−1.291 and 1.462−1.466 Å, respectively.[28] Table 4 shows the energetics of

**Table 4. Free Energies ($\Delta G_{rxn}$(298 K,aq) in kcal/mol) of $O_2^{•−}$ and $HO_2^{•}$ addition to N-tert-Butyl-Substituted PBN Derivatives at the PCM/B3LYP/6-31+G(d,p)//B3LYP/6-31G(d) Level of Theory in Water**

| | free energy of radical addition (kcal/mol) | | | | | |
|---|---|---|---|---|---|---|
| | $O_2^{•−}$ addition | | | $HO_2^{•}$ addition | | |
| nitrone | mono | di | tri | mono | di | tri |
| *α Substitution* | | | | | | |
| PBN-CH₃ | 18.3 | n/a | n/a | −0.9 | n/a | n/a |
| PBN-COOH | 16.8 | 13.1 | 7.5 | 1.7 | 0.5 | 0.1 |
| PBN-C(=O)OMe | 16.3 | 21.9 | 17.2 | 1.9 | 0.5 | 3.1 |
| PBN-C(=O)NH₂ | 15.2 | 14.1 | 14.8 | 4.5 | 4.0 | 3.4 |
| PBN-OMe | 17.7 | 19.3 | 18.3 | −3.1 | −2.9 | −1.0 |
| PBN-OC(=O)Me | 15.8 | 15.2 | a | −1.4 | −3.5 | 2.6 |
| PBN-OC(=O)NHMe | 16.7 | 20.1 | 21.2 | 3.6 | −2.7 | 2.0 |
| PBN-NHC(=O)Me | 12.7 | 11.9 | 6.9 | 0.4 | 0.9 | 0.6 |
| PBN-SMe | 17.2 | 22.4 | 18.3 | −2.2 | 2.0 | 0.0 |
| PBN-P(=O)(OMe)₂ | 20.0 | 28.1 | 24.5 | −0.9 | 0.4 | 3.0 |
| *β Substitution* | | | | | | |
| PBN-CH₂OH | 16.1 | 19.5 | 20.3 | 0.8 | 3.0 | 2.6 |
| PBN-CH₂OC(=O)Me | 16.7 | 24.7 | 12.3 | −4.4 | 1.5 | 1.7 |
| PBN-CH₂NHC(=O)Me | 18.0 | 24.6 | 16.0 | 3.4 | 4.9 | 1.0 |
| PBN-CH₂OC(=O) NHMe | 13.9 | 17.4 | 22.6 | −2.5 | 1.1 | 1.3 |
| PBN-CH₂C(=O)NH₂ | 17.1 | 14.8. | 15.1 | 3.0 | 5.5 | −0.7 |
| PBN-CH₂C(=O)OMe | 17.8 | 20.4 | 18.3 | 0.9 | 5.0 | −0.3 |
| PBN-CH₂OMe | 19.8 | 17.5 | 21.7 | 0.2 | 1.0 | 1.1 |
| PBN-CH₂P(=O) (OMe)₂ | 16.1 | 23.6 | 16.8 | 1.0 | 0.8 | 2.4 |
| PBN-CH₂SMe | 19.7 | 18.6 | 10.3 | −0.2 | 0.9 | 0.6 |

[a]After several attempts to optimize this adduct, only fragmented products were obtained.

$O_2^{•−}$ and $HO_2^{•}$ addition to various mono-, di-, and tri-α- and mono-, di-, and tri-β-substituted PBN derivatives. The majority of the nitrones (22 out of 35) exhibited decreased reactivity of $O_2^{•−}$ and $HO_2^{•}$ as the number of substituents increase from mono- to trisubstitution (Table 4). Only in a few cases did the favorability of radical addition significantly increase with increasing substitution (i.e., from mono- to trisubstitution), such as in the addition of $O_2^{•−}$ to −COOH, −NHC(=O)Me, −CH₂OC(=O)Me, and −CH₂SMe and of $HO_2^{•}$ to −COOH, −NHC(=O)Me, and −CH₂C(=O)NH₂. The reactivities of $O_2^{•−}$ in general are endoergic with −NHC(=O)Me mono-, di-, and trisubstitution being the most favorable with $\Delta G_{rxn}$(298 K) (kcal/mol) values of 12.7, 11.9 and 6.9, respectively. The structures of these $O_2^{•−}$ adducts show intramolecular H-bonding interactions between the amide H and peroxyl O (Figure 5), resulting in proton abstraction of one of the amide H's by the peroxide O to form the hydroperoxyl moiety, similar to that observed for 5-carbamoyl-5-methyl-1-pyrrroline N-oxide (AMPO)[36] with an endoergic $\Delta G_{rxn}$(298 K) value of 6.1 kcal/mol and for diamide-substituted DMPO derivatives with $\Delta G_{rxn}$(298 K) = −3.3 kcal/mol, both of which became the basis for the fast and favorable reactivity of amide-conjugated nitrones in comparison to other spin traps with no such strong
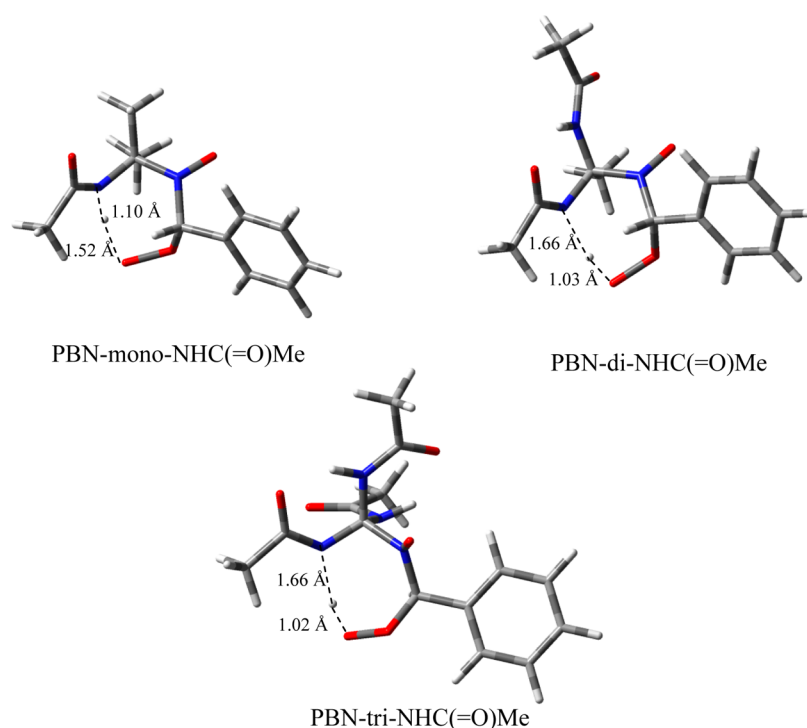
**Figure 5.** Optimized $O_2^{\bullet-}$ adduct structures with the least endoergic free energies of formation, showing the intramolecular H-bond interaction of the amide H with the peroxyl O.

intramolecular interactions.[13,14] The reactivity of $HO_2^{\bullet}$ with nitrones that are monosubstituted with $-CH_2OC(=O)Me$ and disubstituted with $-OCH(=O)Me$ gave the most exoergic free energies of reaction with $\Delta G_{rxn}(298\ K)$ (kcal/mol) of $-4.4$ and $-3.5$, respectively. However, the most exoergic $\Delta G_{rxn}(298\ K)$ (kcal/mol) value observed among all the trisubstituted analogues was only $-1.0$ for the $-OMe$ trisubstitution. Previously, at the same level of theory, we showed that addition of $HO_2^{\bullet}$ to the monoester-substituted EMPO and the diester-substituted DEPO gave the most exoergic $\Delta G_{rxn}(298\ K)$ value of $-6.2$ kcal/mol in comparison to other DMPO derivatives. This suggests that ester conjugation to nitrones is preferred for $HO_2^{\bullet}$ trapping.[37]

The absence of a significant global trend in $HO_2^{\bullet}/O_2^{\bullet-}$ reactivity as a function of increasing nitronyl-C charge density and/or increasing substitution could be accounted for by the competing inductive effects of the methyl group in the partially $\alpha$- and $\beta$-substituted PBN as well as the competing resonance effects of the phenyl ring with the inductive effects of the $\alpha$- and $\beta$-substitution. For mono-$\alpha$-substituted PBN (with the exception of two outliers, $-P(=O)(OMe)_2$ and $-NH(C=O)Me$), a fairly poor correlation ($R^2 = 0.66$) can be observed between the charge densities on the nitronyl C with their respective free energies ($\Delta G_{rxn}(298\ K)$) of addition with $O_2^{\bullet-}$ (Figure S12, Supporting Information). In a similar study involving para substitution on PBN, we showed that there was no correlation that can be observed for $\Delta G_{rxn}(298\ K)$ and nitronyl carbon charge densities in both $O_2^{\bullet-}$ and $HO_2^{\bullet}$ addition reactions.[20] Therefore, the reactivity of $O_2^{\bullet-}$ and $HO_2^{\bullet}$ with mono-$\alpha$-substituted PBN might be similar in nature (i.e., nucleophilic) to those observed for the $O_2^{\bullet-}$ addition to 5-substituted DMPO analogues which are also mono-$\alpha$-substituted,[13] but the effect is much less pronounced, indicating that inductive effect of the substituents for PBN is weaker than that of DMPO analogues. For the mono-$\beta$-substitution, no correlation could be observed with the charge density and their respective $\Delta G_{rxn}(298\ K)$ values

of reactivity with $O_2^{\bullet-}$ (Figure S12), which could be due to the presence of the methylene group that can further diminish the inductive effect by the functional substituent groups.

**Cell Culture and Viability Studies.** Cytoprotective properties of nitrones against $H_2O_2$-induced cell death was investigated in vitro using bovine aortic endothelial cells (BAEC). BAEC were preincubated with varying concentrations ($10-50\ \mu M$) of nitrone derivatives **1**, **2**, and **6–8** (i.e., PBN-CH$_2$OH, PBN-CH$_2$OAc, PBN-CH$_2$OCONHMe, PBN-CH$_2$NHAc, and PBN-(CH$_2$OH)$_2$) and were challenged for 2 h with $H_2O_2$ (1 mM). Extent of cytoprotection was measured using [3-(4,5-dime-thylthiazol-2-yl)-2−5-diphenyltetrazolium-bromide] (MTT) assay. Our results are presented in Figure 6 and show that at $10\ \mu M$ nitrones **2** and **7** exhibited the highest cytoprotection against $H_2O_2$-induced toxicity. At $50\ \mu M$, the protection afforded



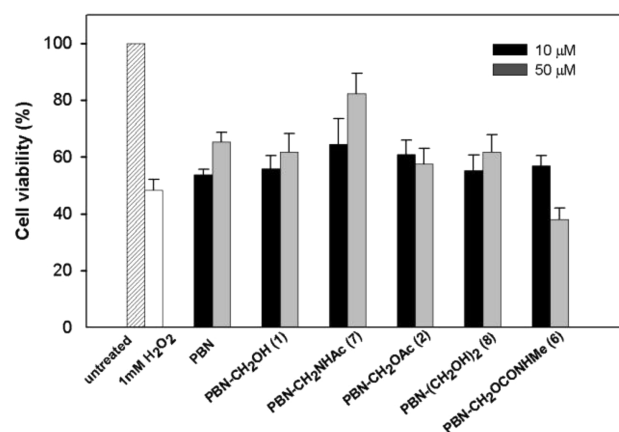**Figure 6.** Cytoprotectivity of PBN derivatives at 10 and 50 $\mu M$ on bovine aortic endothelial cells against 1 mM $H_2O_2$ after 2 h of incubation.

by the nitrones was more pronounced for PBN and compounds **1**, **7** and **8** while for compounds **2** the protection remained similar. A significant decrease of cell viability for compound **6** was noted which was even lower than that of the control and may indicate a slight toxicity due to the carbamate substituent.

To examine the relationship between the electrochemical properties and the antioxidant activities of our derivatives, we tried to correlate the cytoprotection data versus the electrochemical potentials of the nitrones. While no correlation between the reduction potential and the cell viability of nitrone-treated BAEC was observed, a good correlation was observed for the oxidation potentials recorded in acetonitrile with the following order of increasing protective property: PBN-$CH_2OCONHMe$ < PBN-$CH_2OAc$ < PBN-$CH_2OH$ ≈ PBN-$(CH_2OH)_2$ < PBN < PBN-$CH_2NHAc$. Whereas this correlation is particularly obvious at 50 $\mu$M, where increased cytoprotection is inversely correlated with the oxidation potential (Figure 7), at
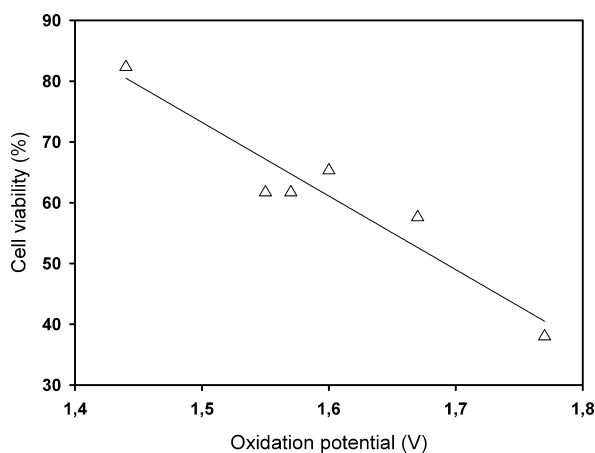


**Figure 7.** Correlation of cell viability with oxidation potential of nitrones **1**, **2**, **6−8**, and PBN in acetonitrile ($R^2 = 0.910$).

10 $\mu$M no correlation was observed (data not shown). It has to be noted that, at 10 $\mu$M, the protection afforded by the nitrones against 1 mM $H_2O_2$ was very limited. This indicates that the ability of nitrones to oxidize at lower potentials offers better cytoprotection, further supporting the role of nitrones in attenuating oxidant-mediated toxicity by an antioxidant mechanism and not solely through spin trapping properties.

## CONCLUSION

In this work, we have studied the electronic effect of various substituents on the reactivity of $\alpha$-phenyl-*N-tert*-butyl nitrones. A series of *N-tert*-butyl-substituted monohydroxyl ($CH_2OH$), monoester ($CH_2OAc$), monoamide ($CH_2NHAc$), and mono-carbamate ($CH_2OCONHMe$) as well as di- and trihydroxyl and di- and triester derivatives was prepared in good yield. The substituent effect on the redox properties was investigated by cyclic voltammetry and showed that electron-withdrawing groups make the nitronyl group more difficult to oxidize. The substituent effect was also demonstrated by a computational approach, where increased positivity on the nitronyl carbons was observed for multiply $\alpha$- and $\beta$-substituted compounds, which correlates well with experimental NMR chemical shifts. A UV−vis stopped-flow kinetic technique was used to demonstrate the nucleophilic nature of superoxide ($O_2^{\bullet-}$) addition to nitrone, in agreement with previous findings on cyclic nitrones. The thermodynamics of $O_2^{\bullet-}$ adduct formation showed that the

reactivity is endoergic in general; however, for $\alpha$-substituted derivatives, a modest correlation was observed with the nitronyl charge density, suggesting a weak nucleophilic nature of $O_2^{\bullet-}$ addition. Moreover, the nucleophilic nature of phenyl radical (Ph$^{\bullet}$) addition to nitrone was also observed using an EPR kinetic method. Finally, a correlation between the cytoprotective property of nitrones against $H_2O_2$-induced cell death and their oxidation potential was observed, indicating that the antioxidant properties are also affected by the nature of the substituent. This study confirms that the electronic effect of the substituents grafted on the *N-tert*-butyl group is of high importance in the design of nitrones with improved trapping and antioxidant properties. Among the nitrones tested, the amide derivative PBN-$CH_2NHAc$ gave the best properties, such as low oxidation potential, good trapping properties, and cytoprotective activity, making the amide bond an efficient linker for *N-tert*-butyl functionalization of the $\alpha$-phenyl *N-tert*-butyl nitrone.

## ■ EXPERIMENTAL SECTION

**Synthesis.** All reagents were from commercial sources and were used as received. All solvents were distilled and dried according to standard procedures. TLC analysis was performed on aluminum sheets coated with silica gel (40−63 $\mu$m). Compound detection was achieved either by exposure to UV light (254 nm) or by spraying a 5% sulfuric acid solution in ethanol or a 2% ninhydrin solution in ethanol and then heating to ∼150 °C. Flash chromatography was carried out on silica gel (40−63 $\mu$m). Size exclusion chromatography was carried out on hydroxypropylated cross-linked dextran. UV/vis spectra were recorded on a UV/vis spectrometer equipped with a double-compartment quartz cell of 10 mm length. Melting points have not been corrected. The $^1$H NMR spectra were recorded at 250 or 400 MHz and the $^{13}$C NMR at 62.86 or 100 MHz. Chemical shifts are given in ppm relative to the solvent residual peak as a heteronuclear reference for $^1$H and $^{13}$C. Abbreviations used for signal patterns are as follows: bs, broad singlet; s, singlet; d, doublet; dd, doublet of doublets; t, triplet; q, quartet; m, multiplet. HR-MS spectra were recorded on a mass spectrometer equipped with a TOF analyzer for ESI+ experiments.

$\alpha$-**Phenyl-*N*-(2-methyl-1-hydoxy-2-propyl) Nitrone (1).** Under an argon atmosphere and with stirring, benzaldehyde (0.80 g, 7.54 mmol), 2-methyl-2-nitro-1-propanol (1.8 g, 15.1 × 10$^{-3}$ mol), and AcOH (2.5 mL, 45.08 mmol) were dissolved in EtOH. The mixture was cooled to 0 °C, and then zinc powder (1.92 g, 29.6 mmol) was slowly added in order to keep the temperature below 15 °C. The mixture was stirred at room temperature for a couple of minutes and then heated to 60 °C in the dark for 10 h in the presence of molecular sieves (4 Å). The reaction mixture was filtered off through a pad of Celite, and the solvent was removed under vacuum. The crude mixture was purified by flash chromatography (EtOAc/cyclohexane 6/4 v/v) followed by two successive crystallizations from EtOAc/*n*-hexane to give compound **3** (0.94 g, 4.87 mmol, 65%) as a white powder: $R_f$ = 0.42 (EtOAc/cyclohexane 8/2 v/v); mp 78.5−78.9 °C; $^1$H NMR (CDCl$_3$, 400 MHz) $\delta$ 8.27 (2H, m), 7.48 (1H, s), 7.43 (3H, m), 4.24−4.27 (1H, t, $J$ = 6.2 Hz), 3.79−3.80 (2H, d, $J$ = 6.0 Hz), 1.61 (6H, s); $^{13}$C NMR (CDCl$_3$, 100 MHz) $\delta$ 132.1, 130.7 (CH), 130.3 (C), 129.2 (CH), 128.5, 72.9 (C), 70.0 (CH$_2$), 23.9 (CH$_3$); UV (MeOH) $\lambda_{max}$ 296 nm; HR-MS (ESI+, *m/z*) calcd for C$_{11}$H$_{15}$NO$_2$ [(M + H)$^+$] 194.1181, found 194.1180. The spectral data of compound **3** were in agreement with those reported by Janzen et al., except for the melting point, which was found to be 75−76 °C.[16]

$\alpha$-**Phenyl-*N*-(2-methyl-1-acetate-2-propyl) Nitrone (2).** With stirring, compound **1** (0.35 g, 1.81 mmol) was dissolved in a Ac$_2$O/pyridine (1/1 v/v) mixture at 0 °C. After 12 h of stirring at room temperature, the mixture was poured into cold 1 N HCl and extracted with CH$_2$Cl$_2$ (3✕). The organic layer was washed with brine, dried over Na$_2$SO$_4$, and concentrated under vacuum. The crude mixture was purified by flash chromatography (cyclohexane/EtOAc 6/4 v/v) to give compound **2** (0.42 g, 1.79 mmol, 98%) as a white oil: $R_f$ = 0.38 (EtOAc/cyclohexane 5/5 v/v); $^1$H NMR (CDCl$_3$, 400 MHz) $\delta$ 8.30 (2H, m),

7.50 (1H, s), 7.43 (3H, m), 4.43 (2H, s), 2.03 (3H, s), 1.62 (6H, s); $^{13}$C NMR (CDCl$_3$, 100 MHz) $\delta$ 170.5 (CO), 130.7 (C), 130.5, 129.0, 128.5 (CH), 72.1 (C), 68.3 (CH$_2$), 23.7, 20.8 (CH$_3$); UV (MeOH) $\lambda_{max}$ 298 nm; HR-MS (ESI+, $m/z$) calcd for C$_{13}$H$_{17}$NO$_3$ [(M + H)$^+$] 236.1286, found 236.1283.

**2-Methyl-2-nitropropyl Methylcarbamate (3).** Under an argon atmosphere and with stirring in a sealed tube, 2-methyl-2-nitro-1-propanol (1 g, 8.39 mmol), DCI (2.11 g, 16.78 mmol), and DMAP (0.102 g, 0.839 mmol) were dissolved in THF under an argon atmosphere. After 2 h of stirring at room temperature, methylamine (1.13 g, 16.78 mmol) was added and the stirring was continued for 18 h. Then, the mixture was filtered and the solvent was removed under vacuum. The crude mixture was purified by flash chromatography (cyclohexane/EtOAc 9/1 v/v) to give compound 3 (1.45 g, 8.23 mmol, 98%) as a white powder: $R_f$ = 0.30 (cyclohexane/EtOAc 8/2 v/v); mp 48.3−49.3 °C; $^1$H NMR (CDCl$_3$, 250 MHz) $\delta$ 4.76 (1H, bs), 4.39 (2H, s), 2.78 (3H, d, $J$ = 4.90 Hz), 1.59 (6H, s); $^{13}$C NMR (CDCl$_3$, 62.86 MHz) $\delta$ 156.0 (CO), 86.7 (C), 68.7 (CH$_2$), 27.6, 23.0 (CH$_3$). HR-MS (ESI+, $m/z$) calcd for C$_6$H$_{13}$N$_2$O$_4$ [(M + H)$^+$] 177.0875, found 177.0878.

**2-Methyl-2-nitropropanamide (5).** The synthetic procedure was essentially the same as for compound 2. 2-Methyl-2-nitropropanamine[38] (3.70 g, 31.50 mmol) was used as the starting material. The crude mixture was purified by flash chromatography (EtOAc/cyclohexane 8/2 v/v) to give compound 5 (4.7 g, 29.16 mmol, 94%) as a white powder: $R_f$ = 0.48 (EtOAc); mp 102.6−103.1 °C; $^1$H NMR (CDCl$_3$, 250 MHz) $\delta$ 6.15 (1H, bs), 3.71 (2H, d, $J$ = 6.6 Hz), 2.00 (3H, s), 1.56 (6H, s); $^{13}$C NMR (CDCl$_3$, 62.86 MHz) $\delta$ 170.7 (CO), 88.8 (C), 46.1 (CH$_2$), 24.0, 23.2 (CH$_3$). HR-MS (ESI+, $m/z$) calcd for C$_6$H$_{13}$N$_2$O$_3$ [(M + H)$^+$] 161.0926, found 161.0927.

**α-Phenyl-N-(2-methyl-1-methylcarbamate-2-propyl) Nitrone (6).** The synthetic procedure was essentially the same as for compound 1. Benzaldehyde (0.30 g, 2.84 mmol) and compound 3 (1 g, 5.67 mmol) were used as starting materials. The crude mixture was purified by flash chromatography (EtOAc/cyclohexane 5/5 v/v) followed by two successive crystallizations from EtOAc/n-hexane to give compound 6 (0.5 g, 2.0 mmol, 70%) as a white powder: $R_f$ = 0.23 (EtOAc/cyclohexane 7/3 v/v); mp 127.8−128.1 °C; $^1$H NMR (CDCl$_3$, 400 MHz) $\delta$ 8.30 (2H, m), 7.48 (1H, s), 7.42−7.43 (3H, m), 4.66 (1H, m), 4.45 (2H, s), 2.76−2.77 (3H, d, $J$ = 4.9 Hz), 1.60 (6H, s); $^{13}$C NMR (CDCl$_3$, 100 MHz) $\delta$ 156.6 (CO), 131.4 (CH), 130.7 (C), 130.4, 128.9, 128.5 (CH), 72.6 (C), 68.5 (CH$_2$), 27.6, 23.6 (CH$_3$); UV (MeOH) $\lambda_{max}$ 298 nm; HR-MS (ESI+, $m/z$) calcd for C$_{13}$H$_{18}$N$_2$O$_3$ [(M + H)$^+$] 251.1395, found 251.1390.

**α-Phenyl-N-(2-methyl-1-acetamide-2-propyl) Nitrone (7).** The synthetic procedure was essentially the same as for compound 1. Benzaldehyde (0.26 g, 2.45 mmol) and compound 5 (0.8 g, 5.0 mmol) were used as starting materials. The crude mixture was purified by flash chromatography (EtOAc) followed by two successive crystallizations from EtOAc/n-hexane to give compound 7 (0.39 g, 1.66 mmol, 68%) as a white powder: $R_f$ = 0.35 (EtOAc/methanol 9.5/0.5 v/v); mp 114.1−114.6 °C; $^1$H NMR (CDCl$_3$, 400 MHz) $\delta$ 8.27 (2H, m), 7.50 (1H, s), 7.44 (3H, m), 6.62 (1H, m), 3.68−3.70 (2H, d, $J$ = 6.3 Hz), 1.98 (3H, s), 1.60 (6H, s); $^{13}$C NMR (CDCl$_3$, 100 MHz) $\delta$ 170.5 (CO), 131.7, 130.7 (CH), 130.4 (C), 129.0, 128.6 (CH), 73.4 (C), 47.3 (CH$_2$), 25.1, 23.3 (CH$_3$); UV (MeOH) $\lambda_{max}$ 298 nm; HR-MS (ESI+, $m/z$) calcd for C$_{13}$H$_{18}$N$_2$O$_2$ [(M + H)$^+$] 235.1446, found 235.1442.

**α-Phenyl-N-(2-methyl-1,3-dihydroxy-2-propyl) Nitrone (8).** The synthetic procedure was essentially the same as for compound 1. Benzaldehyde (0.78 g, 7.40 mmol) and 2-methyl-2-nitro-1,3-propanediol (2 g, 14.80 mmol) were used as starting materials. The crude mixture was purified by flash chromatography (EtOAc) followed by two successive crystallizations from EtOAc/n-hexane to give compound 8 (0.99 g, 4.74 mmol, 65%) as a white powder: $R_f$ = 0.21 (EtOAc); mp 84.2−85.6 °C; $^1$H NMR (CDCl$_3$, 400 MHz) $\delta$ 8.24 (2H, m), 7.52 (1H, s), 7.43 (3H, m), 3.91−3.98 (6H, m), 1.50 (3H, s); $^{13}$C NMR (CDCl$_3$, 100 MHz) $\delta$ 134.7, 131.1 (CH), 129.9 (C), 129.6, 128.6 (CH), 75.9 (C), 66.8 (CH$_2$), 19.3 (CH$_3$); UV (MeOH) $\lambda_{max}$ 296 nm; HR-MS (ESI+, $m/z$) calcd for C$_{11}$H$_{15}$NO$_3$ [(M + H)$^+$] 210.1130, found 210.1126. The spectral data of compound 8 were in agreement with those reported

by Janzen et al.,[16] except for the melting point, which was found to be 52−55 °C.

**α-Phenyl-N-(2-methyl-1,3-di-O-acetyl-2-propyl) Nitrone (10).** The synthetic procedure was essentially the same as for compound 2. Compound 8 (0.40 g, 1.79 mmol) was used as the starting material. The crude mixture was purified by flash chromatography (cyclohexane/EtOAc 4/6 v/v) to give compound 10 (0.25 g, 0.85 mmol, 45%) as a white oil: $R_f$ = 0.27 (EtOAc/cyclohexane 6/4 v/v); $^1$H NMR (CDCl$_3$, 400 MHz) $\delta$ 8.22 (2H, m), 7.41 (1H, s), 7.36 (3H, m), 4.50 (2H, d, $J$ = 11.7 Hz), 4.35 (2H, d, $J$ = 11.7 Hz), 1.98 (6H, s), 1.59 (3H, s); $^{13}$C NMR (CDCl$_3$, 100 MHz) $\delta$ 169.2 (CO), 131.9, 129.8 (CH), 129.3 (C), 128.1, 127.5 (CH), 72.9 (C), 64.3 (CH$_2$), 19.7, 17.8 (CH$_3$); UV (MeOH) $\lambda_{max}$ 298 nm; HR-MS (ESI+, $m/z$) calcd for C$_{15}$H$_{19}$NO$_5$ [(M + H)$^+$] 294.1341, found 294.1337.

**α-Phenyl-N-(2-O-acetylmethyl-1,3-di-O-acetyl-2-propyl) Nitrone (11).** The synthetic procedure was essentially the same as for compound 2. α-Phenyl-N-(2-hydroxymethyl-1,3-dihydroxy-2-propyl) nitrone[17] (0.40 g, 1.77 mmol) was used as the starting material. The crude mixture was purified by flash chromatography (cyclohexane/EtOAc 6/4 v/v) to give compound 11 (0.43 g, 1.22 mmol, 69%) as a white oil: $R_f$ = 0.42 (EtOAc/cyclohexane 5/5 v/v); $^1$H NMR (CDCl$_3$, 400 MHz) $\delta$ 8.28 (2H, m), 7.45 (3H, m), 7.34 (1H, m), 4.61 (6H, s), 2.06 (9H, s); $^{13}$C NMR (CDCl$_3$, 100 MHz) $\delta$ 169.9 (CO), 133.9, 131.1 (CH), 130.0 (C), 129.3, 128.6 (CH), 75.5 (C), 61.4 (CH$_2$), 20.6 (CH$_3$); UV (MeOH) $\lambda_{max}$ 300 nm; HR-MS (ESI+, $m/z$) calcd for C$_{17}$H$_{21}$NO$_7$ [(M + H)$^+$] 352.1396, found 352.1388.

**Determination of Water Solubility.** For PBN and nitrones 6 and 9, a UV calibration curve at 290 nm was established from solutions ranging from $10^{-3}$ to $10^{-2}$ g/L ($R^2 > 0.995$). A saturated solution of nitrone was prepared at 40 °C and then let stand at room temperature overnight. After centrifugation (12000g, 15 min) at room temperature, the concentration of the supernatant solution was determined using the calibration curve. For nitrones 1, 7, and 8, weighed amounts of the nitrone were placed in a vial containing water at room temperature. After each addition, the solution was carefully shaken and the complete dissolution was checked by visual observation.

**Determination of log $k'_W$ Values.** Compounds were dissolved in MeOH at 1.0 mg/mL and were injected onto a C18 reverse phase column (250 mm × 4.6 mm, 5 $\mu$m). The compounds were eluted at various MeOH and water ratios (7/3 to 3/7 v/v) using a flow rate of 0.8 mL/min. The column temperature was 25 °C, and the UV detector wavelength was $\lambda$ 298 nm. Linear regression analysis were performed on three data points for compound 9 (from 5/5 to 3/7; $r^2$ = 0.9996); four points for compound 1 (from 6/4 to 3/7; $r^2$ = 0.9945), compound 8 (from 6/4 to 3/7; $r^2$ = 0.9973), compound 2 (from 7/3 to 4/6; $r^2$ = 0.9957), compound 10 (from 7/3 to 4/6; $r^2$ = 0.9951), compound 11 (from 7/3 to 4/6; $r^2$ = 0.9976); five points for compound 7 (from 7/3 to 3/7; $r^2$ = 0.9936), and compound 6 (from 7/3 to 3/7; $r^2$ = 0.9944). The log $k'$ values were calculated by using the equation: log $k'$ = log(($t - t_0$)/$t_0$), where $t$ is the retention time of the nitrone and $t_0$ is the elution time of MeOH, which is not retained on the column.

**Determination of C log P Values.** The partition coefficient octanol/water ($C$ log $P$) was determined using MarvinSketch 5.9.0, which is available at www.chemaxon.com/marvin.

**Cyclic Voltammetric Measurements.** The electrochemical experiments were carried out using a three-electrode cell under a dry argon atmosphere at room temperature. An Ag/AgCl/saturated NaCl electrode was used as the reference electrode and a platinum wire as the auxiliary electrode. The working electrode (glassy carbon) was polished prior to each experiment using a 0.04 $\mu$m aqueous alumina slurry on a wetted polishing cloth.

**EPR Measurements.** EPR measurements were carried out on a bench EPR spectrometer. The general instrument settings used for spectral acquisition were as follows: microwave power, 10 mW; modulation amplitude, 2 G; received gains, $9 \times 10^1$ to $9 \times 10^2$; scan time, 60 s; sweep width, 99, 147, or 249 G. Spectra were recorded at room temperature, and measurements were performed using a 50 $\mu$L quartz cell or capillary tube for UV or non-UV irradiation experiments, respectively. The spectrum simulation was carried out using the WINSIM program,[39] available as free software from Public Electron

Paramagnetic Resonance Software Tools (http://www.niehs.nih.gov/research/resources/software/tox-pharm/tools/).

**Spin Trapping Studies.** *Hydroxyl Radical Adduct.* To generate the hydroxyl radical, nitrone (20 mM) was dissolved in a Fenton system containing hydrogen peroxide (0.2%), EDTA (2 mM), and iron(II) sulfate (1 mM) in phosphate buffered saline solution.

*Superoxide Radical Adduct. $KO_2$ Generating System.* The superoxide anion radical was generated using different concentrations of nitrones (40 mM for compounds **2** and **6**, 80 mM for compound **10**, and 20 mM for other cases) to a solution of DMSO containing a 20% saturated solution of $KO_2$ in DMSO.

*Pyridine/$H_2O_2$ System.* A pyridine solution of nitrone (20 mM) containing 230 mM $H_2O_2$ was used.

*Methoxy Radical Adduct.* The methoxy radical was generated by adding ∼1 mg of solid $Pb(OAc)_4$ to a DMSO solution of nitrone (25 mM) containing 10% v/v of MeOH.

*Phenyl Radical Adduct.* The phenyl radical was generated by photolysis of a benzene solution of phenyl iodide (3 M), using a xenon discharge lamp (250 W), giving near-UV and visible radiations in the presence of nitrone (50 mM).

**General Computational Methods.** For the addition of each radical species ($O_2^{\bullet-}$ or $HO_2^{\bullet}$) to substituted PBN derivatives, a density functional theory[40,41] computational approach was employed to determine the optimized geometry, vibrational frequencies, and single-point energies of all stationary points.[35,42−44] The effect of aqueous solvation was also investigated using the polarizable continuum model (PCM).[45−49] All calculations were performed using Gaussian 03[50] at the Ohio Supercomputer Center. Single-point energies were obtained at the B3LYP/6-31+G** level[51] on the basis of the optimized B3LYP/6-31G* geometries. Charge and spin densities were obtained from a natural population (NPA)[52] analysis, and percent electron localizations were obtained from natural bond orbital (NBO)[53] analysis at the single-point PCM/B3LYP/6-31+G**//B3LYP/6-31G* level. These calculations used six Cartesian *d* functions. Stationary points for nitrones and their respective adducts have zero imaginary vibrational frequency, as derived from a vibrational frequency analysis (B3LYP/6-31G*). A scaling factor of 0.9806 was used for the zero-point vibrational energy (ZPE) corrections for the B3LYP/6-31G* level.[54] Here, thermal correction to Gibbs free energy was added to the total energy: that is, the sum of total electronic ($\varepsilon_0$) and thermal free ($G_{corr}$) energies with ZPE correction (as outputs from Gaussian) were used for $\Delta G$ value estimation at the 6-31G* level with the solvent effect added at the 6-31+G** level. The $\Delta G$ values of reactions were simply the difference of the sums of these values for the reactants and the products. Spin contamination for all of the stationary points of the radical structures was negligible: i.e., $\langle S^2 \rangle = 0.75$.

**Stopped-Flow Kinetics.** A procedure was followed similar to that of Villamena et al.[13] A solution of $KO_2$-saturated DMF was prepared by adding ∼200 mg of $KO_2$ to 5 mL of DMF under a nitrogen atmosphere. The solution was sonicated and let stand for 5 min. The supernatant (1 mL) was further diluted with 10 mL of DMF to reach a maximum absorbance of ∼3 at 575 nm when it was mixed with 500 $\mu$M phenol red in 90% DMF/10% $H_2O$. This solution was kept on ice and under a nitrogen atmosphere and let stand for 10 min before stopped-flow testing. Solutions of the nitrones and 500 $\mu$M phenol red in 90% DMF/10% $H_2O$ were prepared. A stopped-flow technique consisted of 150 $\mu$L of $KO_2$ solution and 150 $\mu$L of nitrone solution, and the growth and decay of absorption was measured using a UV−vis spectrophotometer rapid mix accessory. The plot was exported to Sigma Plot 11.0, and the absorption increase was fitted to a linear equation ($y = ax + b$). To ensure a constant concentration of $KO_2$ throughout the experiment, a control of $KO_2$ and 500 $\mu$M phenol red was performed both before and after nitrone testing. Each nitrone was tested with four or more concentrations ranging from 5 to 200 mM.

**Spin Trapping Kinetics.** The solvents were of the highest grade of purity commercially available and were used without further purification. The trinitrone TN was synthesized and purified as previously described.[29] Phenyl radical was produced directly in the EPR spectrometer cavity by UV photolysis of a 3 mol $L^{-1}$ iodobenzene solution in benzene. The method of kinetic competition permitted us to evaluate the ratio of the second-order rate constants for the trapping of $Ph^{\bullet}$ by one of the nitrone N of interest ($k_{pN}$, corresponding to the compounds **1**, **2**, and **6−11**) and TN ($k_{-TN}$, used as competitive inhibitor. Then, the commercially available PBN was also tested versus TN in order to determine the ratio of the rate constants for the trapping of $Ph^{\bullet}$ by PBN and by TN: i.e., $k_{pPBN}/k_{TN}$. The concentrations of the various nitrones were varied from 5 to 20 mmol $L^{-1}$, with the $[N]/[TN]$ ratio kept between 1 and 4. For each nitrone, five experiments were repeated twice at $[N]/[TN]$ values equal to 1, 1.6, 2, 3.2, and 4. In each case, a series of 30 EPR spectra was then recorded (scan time for a single spectrum 15 s) on a spectrometer operating at X-band with 100 kHz modulation frequency. The signal-to-noise ratio was improved using an SVD procedure, as described elsewhere.[55] The signal recorded exactly 1.5 min after the beginning of the reaction was then simulated using the Winsim software in order to determine the relative areas of the adducts N-Ph and TN-Ph. In this approach, the ratio $R/r$ was evaluated as follows:

$$\frac{R}{r} = \frac{\text{area of N-Ph signal} + \text{area of TN-Ph signal}}{\text{area of TN-Ph signal}}$$

**Cell Culture and Viability Studies.** Bovine aortic endothelial cells (BAECs) were cultured in T-75 flasks, in Dulbecco's modified eagle medium (DMEM) supplemented with 1 g/L glucose, 10% fetal bovine serum, L-glutamine, 2.5 mg/L of endothelial cell growth supplement, 1% of nonessential amino acids, and 1% of pen/strep at 37 °C under a humidified atmosphere of 5% $CO_2$ and 20% $O_2$. Cells were subcultured after 85−90% confluence. Cytoprotection of $\beta$-substituted nitrones against $H_2O_2$-induced toxicity was assessed via intracellular reduction of MTT (3-(4,5-dimethylthiazol-2-yl)-2,5-diphenyltetrazolium bromide) to its insoluble formazan form. A confluent BAEC culture was seeded onto 96-well plates (∼$1.0 \times 10^4$ cells/well) and incubated for 24 h. BEACs were pretreated with various nitrone concentrations (25, 50, and 100 $\mu$M) and incubated for 24 h. The cells were then incubated in 1 mM hydrogen peroxide for 2 h, followed by the addition of 100 $\mu$L of phosphate buffered saline (PBS) and 50 $\mu$L of MTT solution (5 mg/mL, 5% ethanol) for 1 h. The cells were then incubated in 200 $\mu$L of dimethyl sulfoxide (DMSO) for 2 h. Formazan formation was measured using a microplate reader at 595 nm absorbance. Data were calculated as percent absorbance of untreated cells ± SEM ($n = 5$).

## ■ ASSOCIATED CONTENT

### Ⓢ Supporting Information

Text, figures, and tables giving the complete ref 50, correlation between $\log k'_w$ and $C \log P$, cyclic voltammograms in water and acetonitrile, NPA charge densities and NBO percent electron densities of the nitronyl atoms, NPA charge densities versus free energies of $O_2^{\bullet-}$ addition reactions, ^{1}H NMR and ^{13}C NMR spectra of compounds **1−3**, **5−8**, **10**, and **11**, HRMS spectra of compounds **1−3**, **5−8**, **10**, and **11**, thermodynamic parameters of the nitrones in water at the PCM/B3LYP/6-31+g**//B3LYP/6-31g* level of theory, and Cartesian coordinates. This material is available free of charge via the Internet at http://pubs.acs.org.

## ■ AUTHOR INFORMATION

### Corresponding Authors
*F.A.V.: e-mail, frederick.villamena@osumc.edu; tel, 614-292-8215.
*G.D.: e-mail, gregory.durand@univ-avignon.fr; tel, +33 (0)4 9014 4445.

### Notes

The authors declare no competing financial interest.

## ■ ACKNOWLEDGMENTS

## ■ REFERENCES

(1) Villamena, F. A.; Zweier, J. L. *Antioxid. Redox Signaling* **2004**, *6*, 619.

(2) Dikalova, A. E.; Kadiiska, M. B.; Mason, R. P. *Proc. Natl. Acad. Sci. U.S.A.* **2001**, *98*, 13549.

(3) Kadiiska, M. B.; Burkitt, M. J.; Xiang, Q. H.; Mason, R. P. *J. Clin. Invest.* **1995**, *96*, 1653.

(4) Floyd, R. A.; Kopke, R. D.; Choi, C.-H.; Foster, S. B.; Doblas, S.; Towner, R. A. *Free Radical Biol. Med.* **2008**, *45*, 1361.

(5) Villamena, F. A.; Das, A.; Nash, K. M. *Future Med. Chem.* **2012**, *4*, 1171.

(6) Maples, K. R.; Green, A. R.; Floyd, R. A. *CNS Drugs* **2004**, *18*, 1071.

(7) Hardy, M.; Rockenbauer, A.; Vasquez-Vivar, J.; Felix, C.; Lopez, M.; Srinivasan, S.; Avadhani, N.; Tordo, P.; Kalyanaraman, B. *Chem. Res. Toxicol.* **2007**, *20*, 1053.

(8) Murphy, M. P.; Echtay, K. S.; Blaikie, F. H.; Asin-Cayuela, J.; Cocheme, H. M.; Green, K.; Buckingham, J. A.; Taylor, E. R.; Hurrell, F.; Hughes, G.; Miwa, S.; Cooper, C. E.; Svistunenko, D. A.; Smith, R. A. J.; Brand, M. D. *J. Biol. Chem.* **2003**, *278*, 48534.

(9) Durand, G.; Poeggeler, B.; Ortial, S.; Polidori, A.; Villamena, F. A.; Böker, J.; Hardeland, R.; Pappolla, M. A.; Pucci, B. *J. Med. Chem.* **2010**, *53*, 4849.

(10) Ortial, S.; Durand, G.; Poeggeler, B.; Polidori, A.; Pappolla, M. A.; Boeker, J.; Hardeland, R.; Pucci, B. *J. Med. Chem.* **2006**, *49*, 2812.

(11) Zeghdaoui, A.; Tuccio, B.; Finet, J.-P.; Cerri, V.; Tordo, P. *J. Chem. Soc., Perkin Trans. 2* **1995**, 2087.

(12) Allouch, A.; Roubaud, V.; Lauricella, R.; Bouteiller, J.-C.; Tuccio, B. *Org. Biomol. Chem.* **2003**, *1*, 593.

(13) Villamena, F. A.; Xia, S.; Merle, J. K.; Lauricella, R.; Tuccio, B.; Hadad, C. M.; Zweier, J. L. *J. Am. Chem. Soc.* **2007**, *129*, 8177.

(14) Kim, S.-U.; Villamena, F. A. *J. Phys. Chem. A* **2011**, *116*, 886.

(15) Karoui, H.; Nsanzumuhire, C.; Le Moigne, F.; Hardy, M.; Siri, D.; Derat, E.; Rockenbauer, A.; Ouari, O.; Tordo, P. *Chem. Eur. J.* **2014**, *20*, 4064.

(16) Janzen, E. G.; Zawalski, R. C. *J. Org. Chem.* **1978**, *43*, 1900.

(17) Choteau, F.; Tuccio, B.; Villamena, F. A.; Charles, L.; Pucci, B.; Durand, G. *J. Org. Chem.* **2012**, *77*, 938.

(18) Nollet, L. M. L.; Gelder, L. S. P. D. *Handbook of water analysis*; CRC Press: Boca Raton, FL, 2000.

(19) Buettner, G. *Free Radical Biol. Med.* **1987**, *3*, 259.

(20) Durand, G.; Choteau, F.; Pucci, B.; Villamena, F. A. *J. Phys. Chem. A* **2008**, *112*, 12498.

(21) McIntire, G. L.; Blount, H. N.; Stronks, H. J.; Shetty, R. V.; Janzen, E. G. *J. Phys. Chem.* **1980**, *84*, 916.

(22) Tuccio, B.; Lauricella, R.; Frejaville, C.; Bouteiller, J.-C.; Tordo, P. *J. Chem. Soc., Perkin Trans. 2* **1995**, 295.

(23) Zuman, P.; Exner, O. *Collect. Czech. Chem. Commun.* **1965**, *30*, 1832.

(24) Tuccio, B.; Bianco, P.; Bouteiller, J.-C.; Tordo, P. *Electrochim. Acta* **1999**, *44*, 4631.

(25) Acken, B. J.; Gallis, D. E.; Warshaw, J. A.; Crist, D. R. *Can. J. Chem.* **1992**, *70*, 2076.

(26) Nakahara, K.; Iwasa, S.; Iriyama, J.; Morioka, Y.; Suguro, M.; Satoh, M.; Cairns, E. J. *Electrochim. Acta* **2006**, *52*, 921.

(27) Suryanarayanan, V.; Yoshihara, S.; Shirakashi, T. *Electrochim. Acta* **2005**, *51*, 991.

(28) Villamena, F. A.; Dickman, M. H.; Crist, D. R. *Inorg. Chem.* **1998**, *37*, 1446.

(29) Roubaud, V.; Dozol, H.; Rizzi, C.; Lauricella, R.; Bouteiller, J.-C.; Tuccio, B. *J. Chem. Soc., Perkin Trans. 2* **2002**, 958.

(30) Lauricella, R.; Bouteiller, J.-C.; Tuccio, B. *Phys. Chem. Chem. Phys.* **2005**, *7*, 399.

(31) Sueishi, Y.; Yoshioka, C.; Olea-Azar, C.; Reinke, L. A.; Kotake, Y. *Bull. Chem. Soc. Jpn.* **2002**, *75*, 2043.

(32) Sueishi, Y.; Yoshioka, D.; Yoshioka, C.; Yamamoto, S.; Kotake, Y. *Org. Biomol. Chem.* **2006**, *4*, 896.

(33) Abe, Y.; Seno, S.; Sakakibara, K.; Hirota, M. *J. Chem. Soc., Perkin Trans. 2* **1991**, 897.

(34) Murofushi, K.; Abe, K.; Hirota, M. *J. Chem. Soc., Perkin Trans. 2* **1987**, 1829.

(35) DeVleeschouwer, F.; VanSpeybroeck, V.; Waroquier, M.; Geerlings, P.; DeProft, F. *Org. Lett.* **2007**, *9*, 2721.

(36) Villamena, F. A.; Rockenbauer, A.; Gallucci, J.; Velayutham, M.; Hadad, C. M.; Zweier, J. L. *J. Org. Chem.* **2004**, *69*, 7994.

(37) Villamena, F. A.; Merle, J. K.; Hadad, C. M.; Zweier, J. L. *J. Phys. Chem. A* **2007**, *111*, 9995.

(38) Durand, G.; Polidori, A.; Ouari, O.; Tordo, P.; Geromel, V.; Rustin, P.; Pucci, B. *J. Med. Chem.* **2003**, *46*, 5230.

(39) Duling, D. R. *J. Magn. Reson., Ser. B* **1994**, *104*, 105.

(40) Labanowski, J. W.; Andzelm, J. *Density Functional Methods in Chemistry*; Springer: New York, 1991.

(41) Parr, R. G.; Yang, W. *Density Functional Theory in Atoms and Molecules*; Oxford University Press: New York, 1989.

(42) Becke, A. D. *Phys. Rev.* **1988**, *38*, 3098.

(43) Becke, A. D. *J. Chem. Phys.* **1993**, *98*, 1372.

(44) Hehre, W. J.; Radom, L.; Schleyer, P. V.; Pople, J. A. *Ab Initio Molecular Orbital Theory*; Wiley-Interscience: New York, 1986.

(45) Barone, V.; Cossi, M.; Tomasi, J. *J. Chem. Phys.* **1997**, *107*, 3210.

(46) Barone, V.; Cossi, M.; Tomasi, J. *J. Comput. Chem.* **1998**, *19*, 404.

(47) Cossi, M.; Barone, V.; Cammi, R.; Tomasi, J. *Chem. Phys. Lett.* **1996**, *255*, 327.

(48) Tomasi, J.; Mennucci, B.; Cammi, R. *Chem. Rev.* **2005**, *105*, 2999.

(49) Tomasi, J.; Persico, M. *Chem. Rev.* **1994**, *94*, 2027.

(50) Frisch, M. J. ,et al. *Gaussian 03, Revision B.04 ed.*; Gaussian, Inc.: Pittsburgh, PA, 2003.

(51) Lee, C.; Yang, W.; Parr, R. G. *Phys. Rev. B* **1988**, *37*, 785.

(52) Reed, A. E.; Curtiss, L. A.; Weinhold, F. A. *Chem. Rev.* **1988**, *88*, 899.

(53) Foster, J. P.; Weinhold, J. *J. Am. Chem. Soc.* **1980**, *102*, 7211.

(54) Scott, A. P.; Radom, L. *J. Phys. Chem.* **1996**, *100*, 16502.

(55) Lauricella, R.; Allouch, A.; Roubaud, V.; Bouteiller, J.-C.; Tuccio, B. *Org. Biomol. Chem.* **2004**, *2*, 1304.